



Title	Numerical simulation of screening current distribution in HTS tape of high field magnet
Author(s)	Itoh, Ryusei; Oga, Yuki; Noguchi, So; Igarashi, Hajime; Ueda, Hiroshi
Citation	Physica C : Superconductivity and its Applications, 484, 300-304 https://doi.org/10.1016/j.physc.2012.03.040
Issue Date	2013-01
Doc URL	http://hdl.handle.net/2115/52755
Type	article (author version)
File Information	SAP51_ISS2011_revised.pdf



[Instructions for use](#)

SAP-51 / ISS2011

Submitted 30 November 2011

Numerical simulation of screening current distribution in HTS tape of high field magnet

R. Itoh^a, Y. Oga^a, S. Noguchi^{a,*}, H. Igarashi^a, H. Ueda^b

^aGraduate School of Information Science and Technology, Hokkaido University, Kita 14 Nishi 9, Kita-ku, Sapporo 060-0814, Japan.

^bResearch Center for Nuclear Physics, Osaka University, 10-1 Mihogaoka, Ibaraki, Osaka 567-0047, Japan.

Abstract

In recent years, properties of high temperature superconducting (HTS) tapes, especially in-field performance and mechanical strength, have been continuously improved. The HTS tapes have been widely used for high field (>20 T) magnet researches and there are several technical challenges including field attenuation of an HTS magnet by screening currents induced within the HTS tapes. Several publications reported that the screening currents, induced by penetration of self magnetic fields into

HTS tapes within an HTS magnet, weakened a field constant of the HTS magnet. The result may demonstrate that the screening current changes an overall current density distribution in HTS tapes and, as a consequence, the generated magnetic field. Therefore, it is necessary to investigate the screening current distribution in an HTS tape. This paper reports numerical simulation of the screening current distribution in an HTS tape of high field magnets using 2D finite element method with the E - J characteristic of the HTS tape taken into account. Self magnetic field distribution and its orientation to the HTS tape are also considered to compute critical currents and locally generated electric fields, two key components to figure out the distribution of screening currents.

PACS code: 84.71.Ba, 84.71.Mn

Keywords: High field superconducting magnet; high temperature superconducting tape; screening current; E - J characteristic

*Corresponding author

Prof. So Noguchi

Graduate School of Information Science and Technology, Hokkaido University

Kita 14 Nishi 9, Kita-ku, Sapporo 060-0814, Japan

Phone: +81-11-706-7671

Fax: +81-11-706-7670

E-mail: noguchi@ssi.ist.hokudai.ac.jp

1. Introduction

In an HTS (High Temperature Superconducting) magnet, especially wound with "tape-shaped" conductors, perpendicular components of generated magnetic fields induce screening currents in HTS conductors. On the other hand, the screening currents are hardly induced in MgB₂ conductors since the cross-section of MgB₂ conductors is generally round with a very small diameter. When a total current consisting of screening and transport currents exceeds a critical current in a local spot of the HTS conductor, an electrical resistance appears according to E - J characteristics of the HTS conductor though the transport current does not exceed the critical current. The appearance electrical resistance attenuates the transport current, and then it also decreases the magnetic field [1-3]. Consequently, it is difficult to generate a desired magnetic field and to predict a generated magnetic field unless the power supply keeps connecting to the HTS magnet. It is, therefore, important to investigate the screening current distribution .

To investigate such a phenomenon, we have developed a simulation code to compute the distribution of screening current and transport current for HTS magnets wound HTS tapes. The developed code was based on a 2D finite element method (FEM) and the Biot-Savart law.

2. Simulation Method

The governing equation for computing current density distribution in an HTS tape is as follows:

$$\text{rot } \mathbf{E} = -\frac{\partial \mathbf{B}}{\partial t} \quad (1)$$

where \mathbf{E} and \mathbf{B} are the electric field and the magnetic field, respectively. Introducing current vector potential \mathbf{T} ($\mathbf{E} = \rho \text{rot} \mathbf{T}$), Eq. (1) yields

$$\text{rot}(\rho \text{rot} \mathbf{T}) = -\frac{\partial \mathbf{B}}{\partial t} \quad (2)$$

where ρ is the equivalent electrical resistivity of high T_c superconductor. Here, the HTS tape is thin enough so that it is possible to consider the current density distribution as a 2D phenomenon. Consequently, using the z -component of the current vector potential T_z and the magnetic field B_z , Eq. (2) yields

$$-\frac{\partial}{\partial x} \rho \frac{\partial T_z}{\partial x} - \frac{\partial}{\partial y} \rho \frac{\partial T_z}{\partial y} = -\frac{\partial B_z}{\partial t}. \quad (3)$$

In addition, the current vector potential separates to those caused by the transport current T_t and the screening current T_s ($T_z = T_t + T_s$).

$$-\frac{\partial}{\partial x} \rho \frac{\partial (T_t + T_s)}{\partial x} - \frac{\partial}{\partial y} \rho \frac{\partial (T_t + T_s)}{\partial y} = -\frac{\partial B_{\perp}}{\partial t} \quad (4)$$

where B_{\perp} is the magnetic field perpendicular to the HTS tape surface. The HTS tape is

thin enough so that it is supposed that the transport current I is not influenced by time-varying magnetic field. Consequently, Eq. (4) can be divided to

$$-\frac{\partial}{\partial x}\rho\frac{\partial T_t}{\partial x}-\frac{\partial}{\partial y}\rho\frac{\partial T_t}{\partial y}=0, \text{ and} \quad (5)$$

$$-\frac{\partial}{\partial x}\rho\frac{\partial T_s}{\partial x}-\frac{\partial}{\partial y}\rho\frac{\partial T_s}{\partial y}=-\frac{\partial B_{\perp}}{\partial t}. \quad (6)$$

Eqs. (5) and (6) are separately solved by the 2D FEM, where the electrical resistivity ρ is computed by taking into account the E - J characteristic based on the percolation model [4]. The perpendicular self magnetic field B_{\perp} is computed based on the Biot-Savart law.

The transport current I is attenuated by the electrical resistance R which is calculated from the equivalent electrical resistivity ρ , according to the following equation

$$L\frac{dI}{dt}+RI=0 \quad (7)$$

where L is the coil inductance, and the transport current I is computed from

$$I=\int_A \text{rot}T dS, \text{ where } A \text{ is the cross-sectional area of the HTS tape.}$$

In the simulation, Eqs. (5), (6), and (7) are simultaneously solved with the nonlinear equivalent electrical resistivity ρ .

3. HTS Coil Models

For investigation of the screening current, Figs. 1 and 2 show the shape of HTS coils (A and B), which were revealed as HTS coils with a large and a small attenuation of

magnetic field in Ref. [1]. The HTS coils are wound with YBCO tape, whose specifications are shown in Table 1, and Fig. 3 shows the J_c - B - θ characteristic of the HTS tape used in this paper.

The HTS coil *A* has 5 layers and 72 turns each layer as shown in Fig. 1. Table 2 shows the specifications of the HTS coil *A*. The critical current I_c is 244 A, and Fig. 4 shows the distribution of the magnetic field generated by the HTS coil *A* at $I = I_c$. Fig. 5 shows the magnetic field perpendicular to the HTS tape surface at $I = I_c$, which corresponds to the radial component of the magnetic field generated by the HTS coil *A*. The screening current of the middle layer of the HTS coil *A* hardly flows because the magnetic flux does not penetrate the HTS tape in total. Therefore, the current simulation in only the first and the second bottom layer was carried out in the case of the HTS coil *A*.

The HTS coil *B* has 2 layers and 248 turns each layer as shown in Fig. 2, and the specifications of the HTS coil *B* is shown in Table 3. Fig. 6 shows the magnetic field perpendicular to the HTS tape surface at $I = 256$ A ($= I_c$). It is well known that a flat shape of HTS coil prevents a large magnetic field from penetrating the HTS tape surface [4]. Therefore, a small screening current in HTS coil *B* would be induced as compared to HTS coil *A* [1]. The current simulation in only the bottom layer was carried out

because of the symmetry.

4. Simulation Results and Discussion

4.1 HTS Coil A with Large Attenuation of Magnetic Field

In the simulation, the transport current increases to ($I_{\text{peak}} =$) 220 A, the HTS coil A generates ($B_0 =$) 2.63 T at magnet center. Fig. 7 shows the time-varying transport current I and the coil resistance R . As shown in Fig. 7, it is observed that the transport current attenuates 28.6%. The electrical resistance of the HTS tape begins to appear at $I = 205$ A. Although the critical current I_c is 244 A, the transport current finally converges to ($I_f =$) 157 A. Fig. 8 shows the time-varying center magnetic field B_0 . The center magnetic field also attenuates 28.6%. However, it is seemed that the decrease of the transport current is too fast. It is strongly dependent on a coil inductance L and E - J characteristics, so more investigations are necessary with respect to the E - J characteristics.

In the next simulations, the peak transport current I_{peak} of 210 and 250 A are also investigated, and these results are also shown in Fig. 7. In the case of $I_{\text{peak}} = 210$ A, the reduction of the transport current is small due to a small electrical resistance. On the other hands, a large electrical resistance appears since the current of 250 A exceeds the critical current of HTS coil A. However, the convergent transport current I_f is 155 A

similar to that of the peak transport current I_{peak} of 220 A.

Fig. 9 shows the distribution of the screening current density J_s in the HTS tape of coil A in the case of $I_{\text{peak}} = 220$ A. From Fig. 9, it is obvious that a larger screening current on the first bottom layer flows than that on the second bottom layer. When the transport current reaches to 219 A ($t = 21.9$ s), the large screening current locally flows along the top and the bottom edge of the HTS tape, as shown in Fig. 9 (a). The net current density consisting of the screening and the transport current exceeds the critical density in the local area, so that the electrical resistance appears. While the transport current is attenuating, the screening current flows in the opposite direction, as shown in Fig. 9 (b), since the direction of change of the magnetic field alternates. The electrical resistance continuously appears on the same way. During the attenuation of the transport current, the screening current is large enough so that the transport current decreases below the critical current. And then, when the electrical resistance and the screening current is small enough the attenuation of the transport current stops, as shown in Fig. 9 (c).

The attenuation of the center magnetic field is revealed in the simulation results. When an HTS coil is charged close to a critical current, a screening current is induced and then an electrical resistance appears. Because of the electrical resistance the

transport current attenuates. The attenuating transport current varies the magnetic field penetrating into the HTS tape surface. The time-varying magnetic field again generates the screening current and the electrical resistance. Consequently, the transport current converges below the critical current. The larger the transport current flows, the larger the transport current is reduced. Fig. 10 and Table 4 show the converged value I_f of the transport current and the reduction rate η .

4.2 HTS Coil B with Small Attenuation of Magnetic Field

When the transport current increases to ($I_{\text{peak}} =$) 220 A, the HTS coils B also generates 2.63 T at magnet center [1]. Fig. 11 shows the time-varying transport current I and the coil resistance R . The transport current of HTS coil B converges to 160 A, the reduction rate η is 27.3%. The electrical resistance appears at $I = 207$ A in the case of HTS coil B . As shown in Fig. 11, it is observed that the transport current of the HTS coil B attenuates smaller than that of the HTS coil A . However, a large electrical resistance of the HTS coil B appears due to the long HTS tape (49.77 m). The large coil inductance of HTS coil B keep the transport current higher as compared to the HTS coil A .

Fig. 12 shows the distribution of the screening current density J_s in the HTS tape of coil B . When the transport current I reaches to 219 A ($t = 21.9$ s), the large screening current locally flows along the bottom edge of the HTS tape, as shown in Fig. 12 (a).

The net current density, which consists of the screening and the transport current, exceeds the critical current density on the bottom edge, so that the large electrical resistance appears. While the transport current is attenuating, the screening current also flows in the opposite direction, as shown in Fig. 12 (b). During the attenuation of the transport current, the screening current is large enough so that the transport current decreases below the critical current. And then, when the electrical resistance and the screening current is small enough the attenuation of the transport current stops, as shown in Fig. 12 (c).

The screening current density of HTS coil *B* is slightly smaller than that of HTS coil *A*, comparing Fig. 9 (a) to Fig. 12 (a). It is apparent that the screening current depends on the shape of HTS coil. However, a reduction rate of transport current depends on an electrical resistance resulting from the screening current as well as a coil inductance.

5. Conclusion

The simulation of screening currents was carried out using the 2D finite element method. The screening current and the transport current were separately formulated because the screening current was dependent on temporal variation of magnetic field while the transport current was not. With the large aspect ratio of thin HTS tapes taken into consideration, the HTS tapes were modeled in a 2-D way.

In simulation, a transport current, which was assumed to be supplied from a constant voltage mode power source, attenuates due to an electrical resistance that appears at a local spot within an HTS magnet when a total current consisting of the transport and the screening currents exceeds a critical current at the local area. The electrical resistance causes the attenuation of the transport current and thereby the transport current decreases below the critical current of HTS coil. It is apparent that the larger the transport current flows, the larger the reduction of the transport current is. Moreover, the screening current depends on the shape of HTS coil and the reduction rate of the transport current depends on the electrical resistance resulting from the screening current as well as the inductance of HTS coil.

In future, it is necessary to investigate the relationship between E - J characteristic and screening current. It is also necessary to investigate influence of final current density distribution on homogeneity of a magnetic field for MRI and NMR. In addition, a design method of HTS coil should be developed to reduce the screening current.

References

- [1] Y. Yanagisawa, H. Nakagome, D. Uglietti, T. Kiyoshi, R. Hu, T. Takematu, T. Takao, M. Takahashi, H. Maeda, IEEE Trans. Appl. Supercond. 20 (2010) 744.

- [2] Y. Yanagisawa, Y. Kominato, H. Nakagome, R. Hu, T. Takematsu, T. Takao, D. Uglietti, T. Kiyoshi, M. Takahashi, H. Maeda, IEEE Trans. Appl. Supercond. 21 (2011) 1640.
- [3] M. C. Ahn, T. Yagai, S. Hahn, R. Ando, J. Bascunan, Y. Iwasa, IEEE Trans. Appl. Supercond. 19 (2009) 2269.
- [4] K. Yamafuji, T. Kiss, Physica C, 258 (1996) 197.
- [5] S. Noguchi, A. Ishiyama, S. Akita, H. Kasahara, Y. Tatsuta, S. Kouso, IEEE Trans. Appl. Supercond. 15 (2005) 1927.

Figure captions

Fig. 1. Schematic view of the HTS coil *A*, which has 5 layers and 72 turns each layer.

The HTS coil *A* is shown as an HTS coil with a large screening current in Ref. [1]. The HTS tape of the first and second bottom layers are analyzed by 2D FEM.

Fig. 2. Schematic view of the HTS coil *B*, which has 2 layers and 248 turns each layer.

The HTS coil *B* is shown as an HTS coil with a small screening current in Ref. [1]. The HTS tape of the first bottom layer is analyzed by 2D FEM.

Fig. 3. J_c - B - θ characteristic of HTS tape used in this paper at temperature $T = 20$ K.

Fig. 4. Magnetic field distribution generated by the HTS coil *A* at $I = 244$ A.

Fig. 5. Magnetic field distribution perpendicular to the HTS tape surface in the case of HTS coil *A* at $I = 244$ A. The width direction is enlargedly depicted.

Fig. 6. Magnetic field distribution perpendicular to the HTS tape surface in the case of HTS coil *B* at $I = 256$ A. The width direction is enlargedly depicted.

Fig. 7. Time transition of the transport current I and the electrical resistance R in the case of HTS coil A , where the peak transport currents I_{peak} are 210, 220, and 250 A.

Fig. 8. Time transition of the magnetic field at center of HTS coil A at the peak transport current I_{peak} of 220 A.

Fig. 9. Screening current distribution of HTS coil A at (a) $t = 21.9$ s, (b) $t = 22.8$ s, and (c) $t = 28.0$ s in the case of $I_{\text{peak}} = 220$ A. The width direction is enlargedly depicted.

Fig. 10. Converged value I_f of the transport current and reduction rate η in the case of HTS coil A .

Fig. 11. Time transition of the transport current I and the electrical resistance R in the case of HTS coils A and B , where the peak transport current I_{peak} is 220 A.

Fig. 12. Screening current distribution of HTS coil B at (a) $t = 21.9$ s, (b) $t = 22.8$ s, and (c) $t = 28.0$ s. The width direction is enlargedly depicted.

Tables

Table 1 Specifications of HTS tape

Width of YBCO tape (mm)	4.0
Thickness of YBCO tape (mm)	0.1
Thickness of YBCO layer (μm)	1.0

Table 2 Specifications of HTS coil A

Outer diameter (mm)	40.0	Number of layers	5
Inner diameter (mm)	18.0	Number of turns each layer	72
Length of coil (mm)	25.0	Total simulated length of YBCO tape (m)	13.28
Coil inductance L (mH)	2.0	Critical current I_c (A)	244
Number of turns	360	Operating temperature (K)	20

Table 3 Specifications of HTS coil B

Outer diameter (mm)	109.0	Number of layers	2
Inner diameter (mm)	18.0	Number of turns each layer	248
Length of coil (mm)	8.3	Total simulated length of YBCO tape (m)	49.77
Coil inductance L (mH)	11.0	Critical current I_c (A)	256
Number of turns	496	Operating temperature (K)	20

Table 4 Attenuation characteristic of transport current of HTS coil A

Peak current I_{peak} (A)	Converged value I_f (A)	Reduction rate η (%)
210	164	21.9
220	157	28.6
250	155	38.0

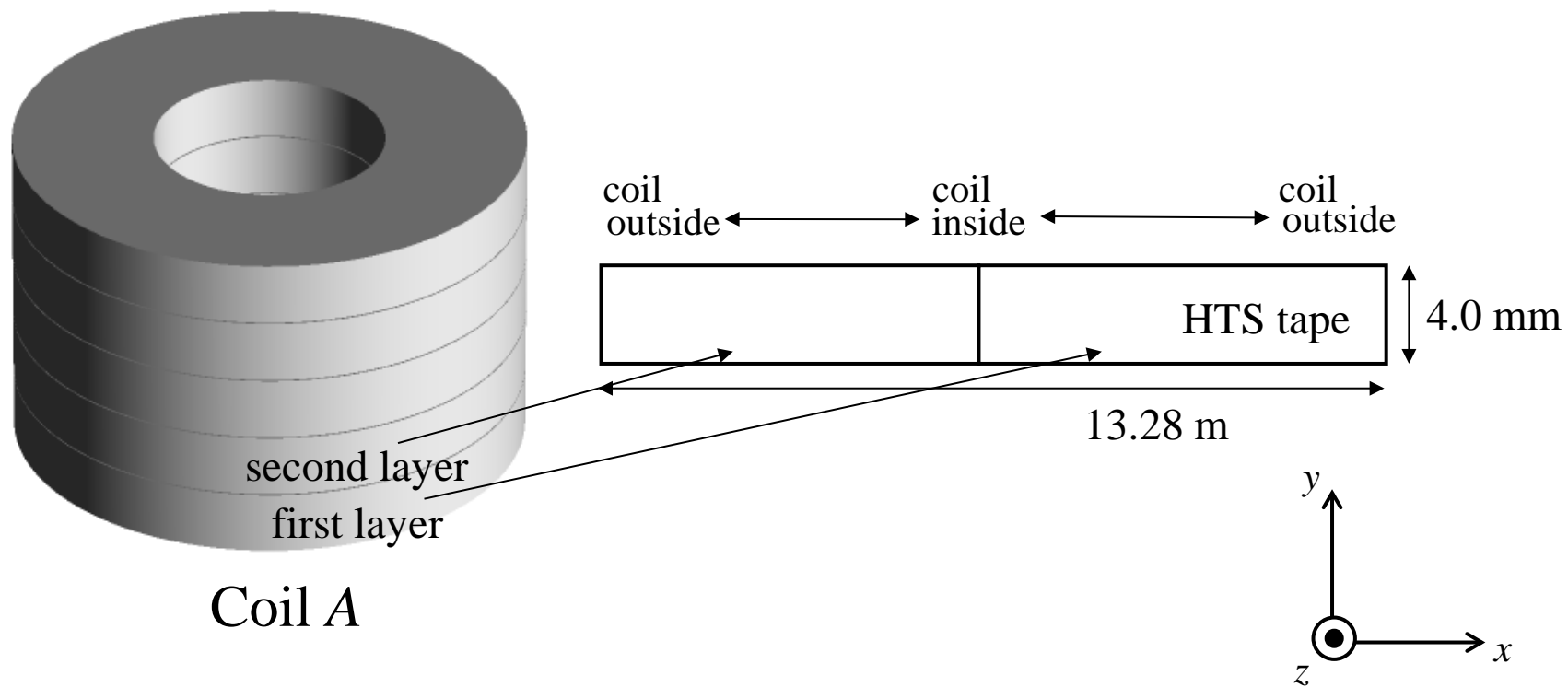


Fig. 1
SAP-51

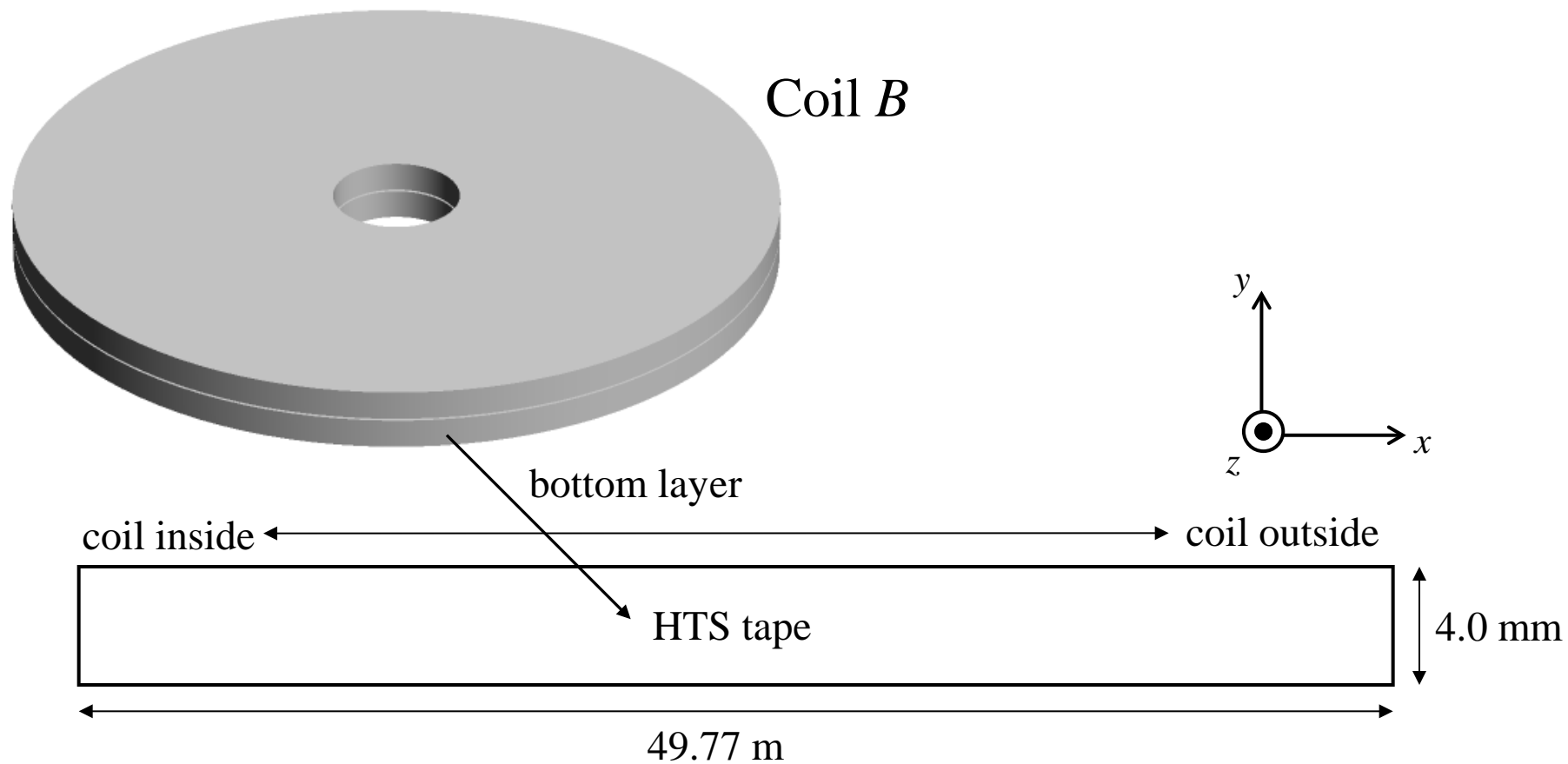


Fig. 2
SAP-51

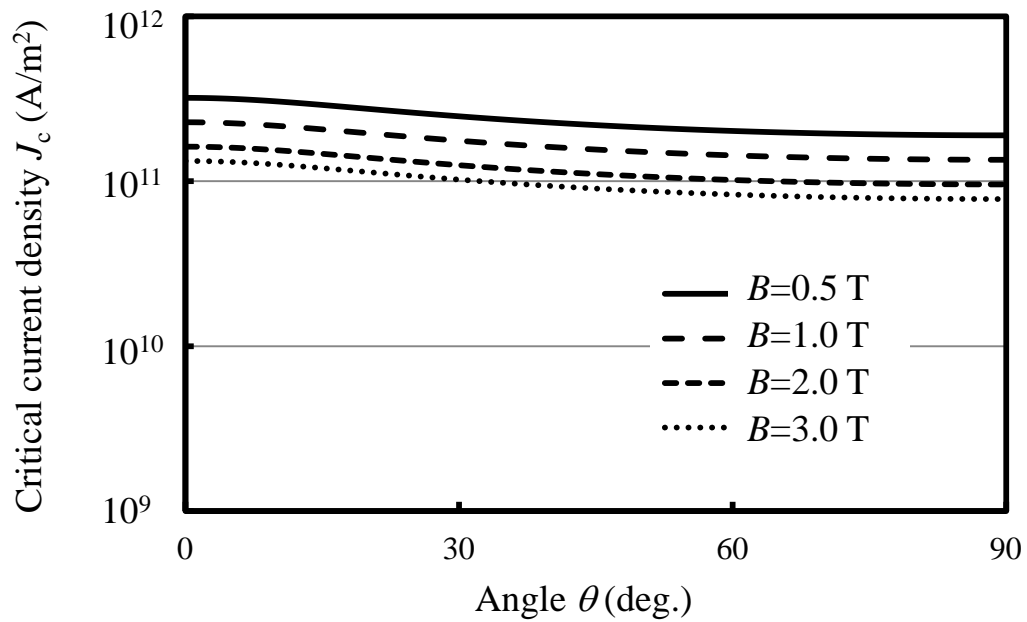


Fig. 3
SAP-51

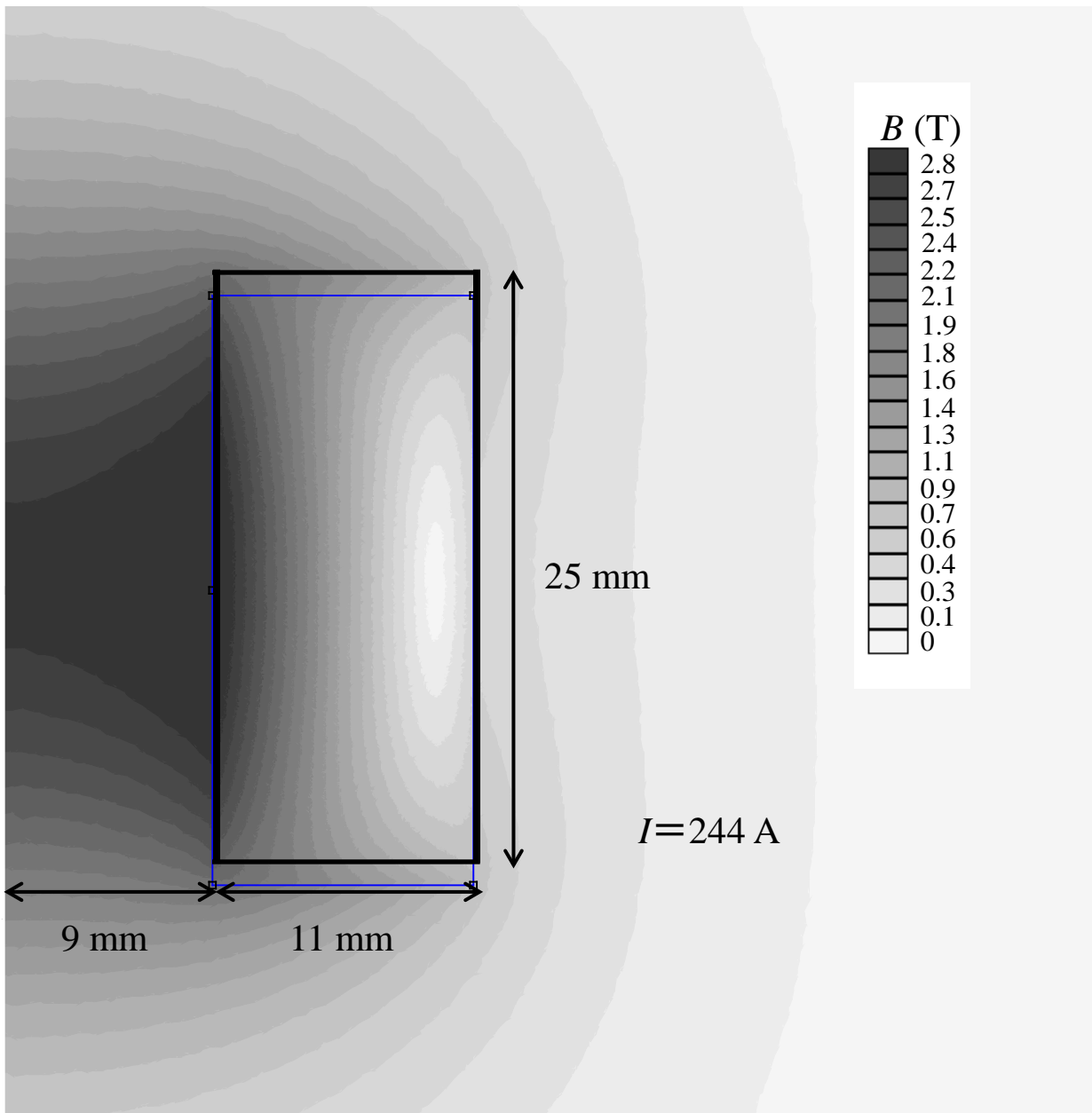


Fig. 4
SAP-51

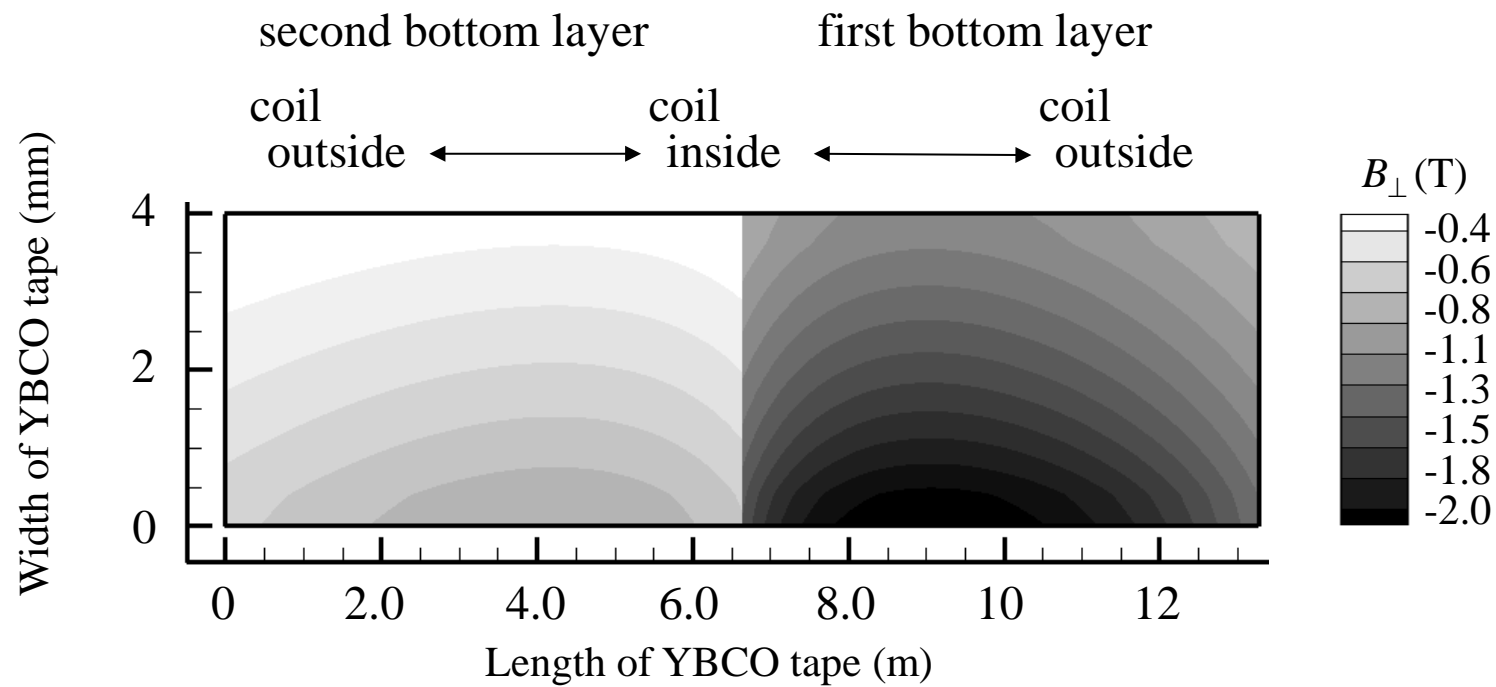


Fig. 5
SAP-51

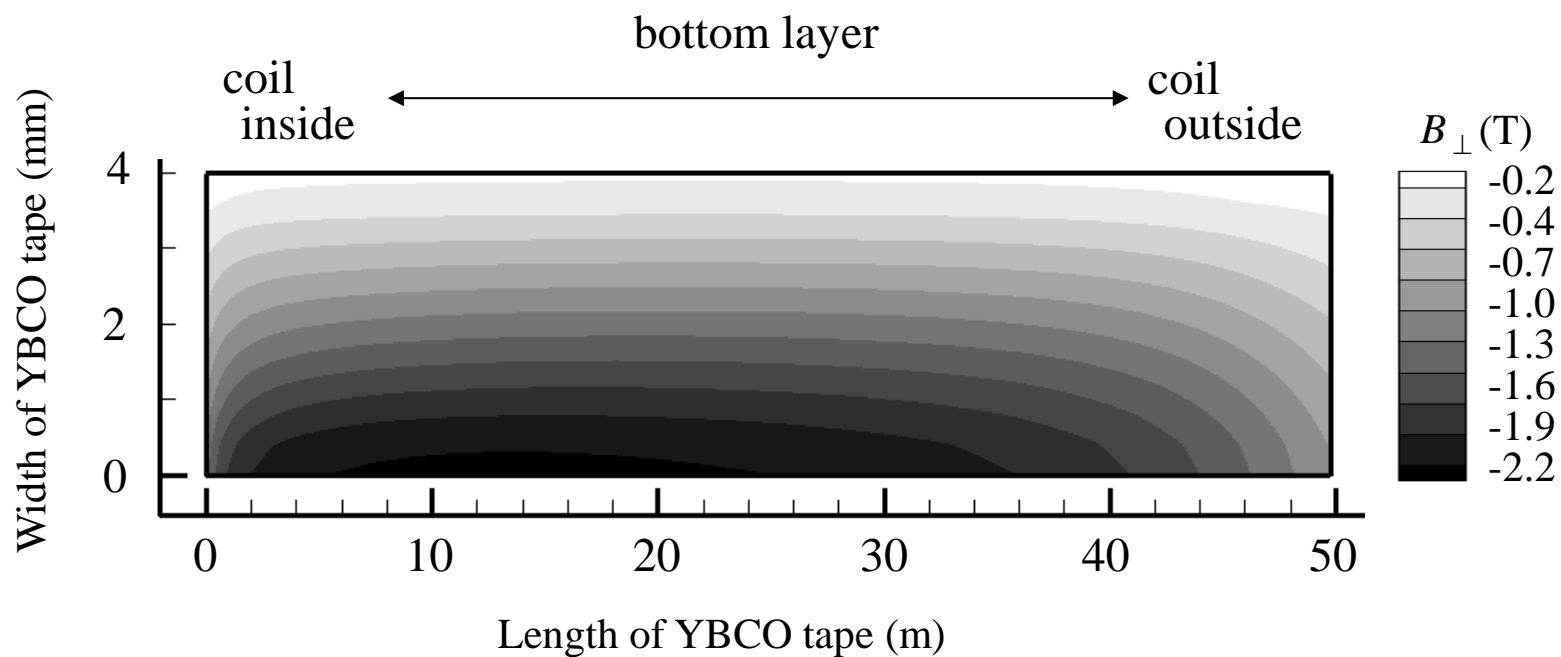


Fig. 6
SAP-51

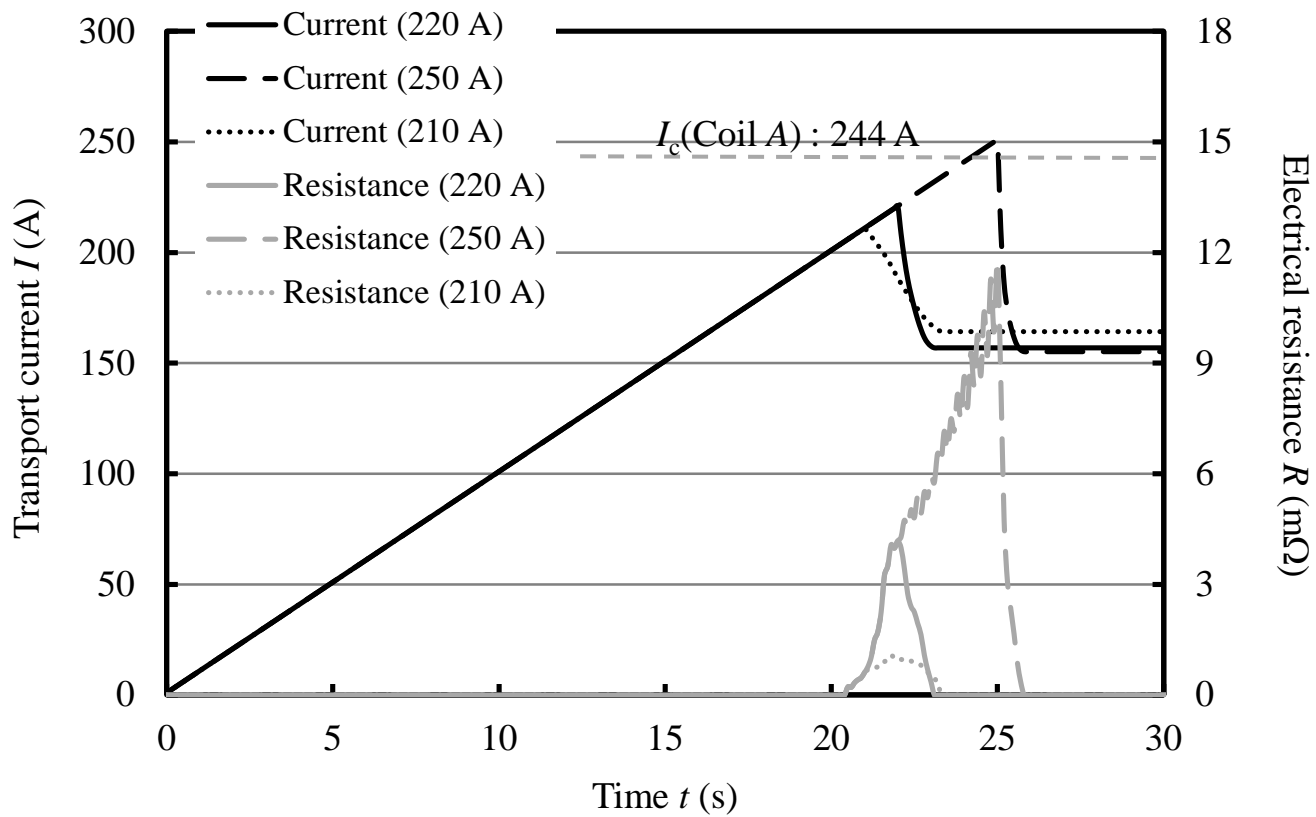


Fig. 7
SAP-51

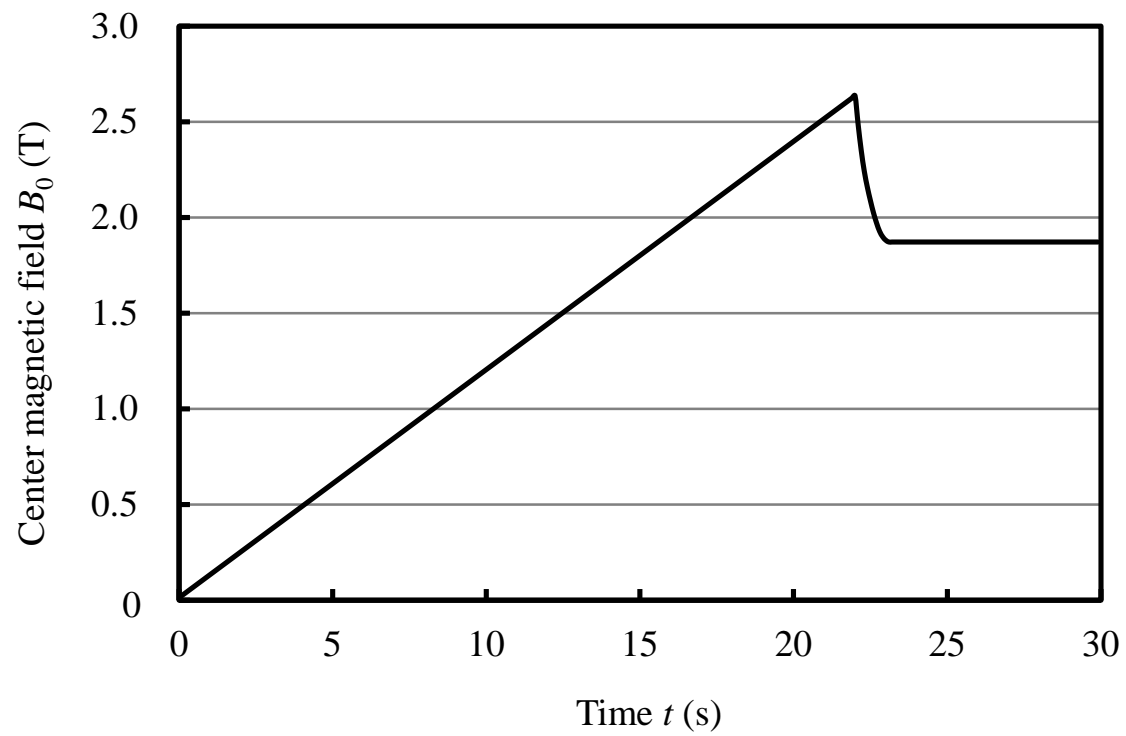


Fig. 8
SAP-51

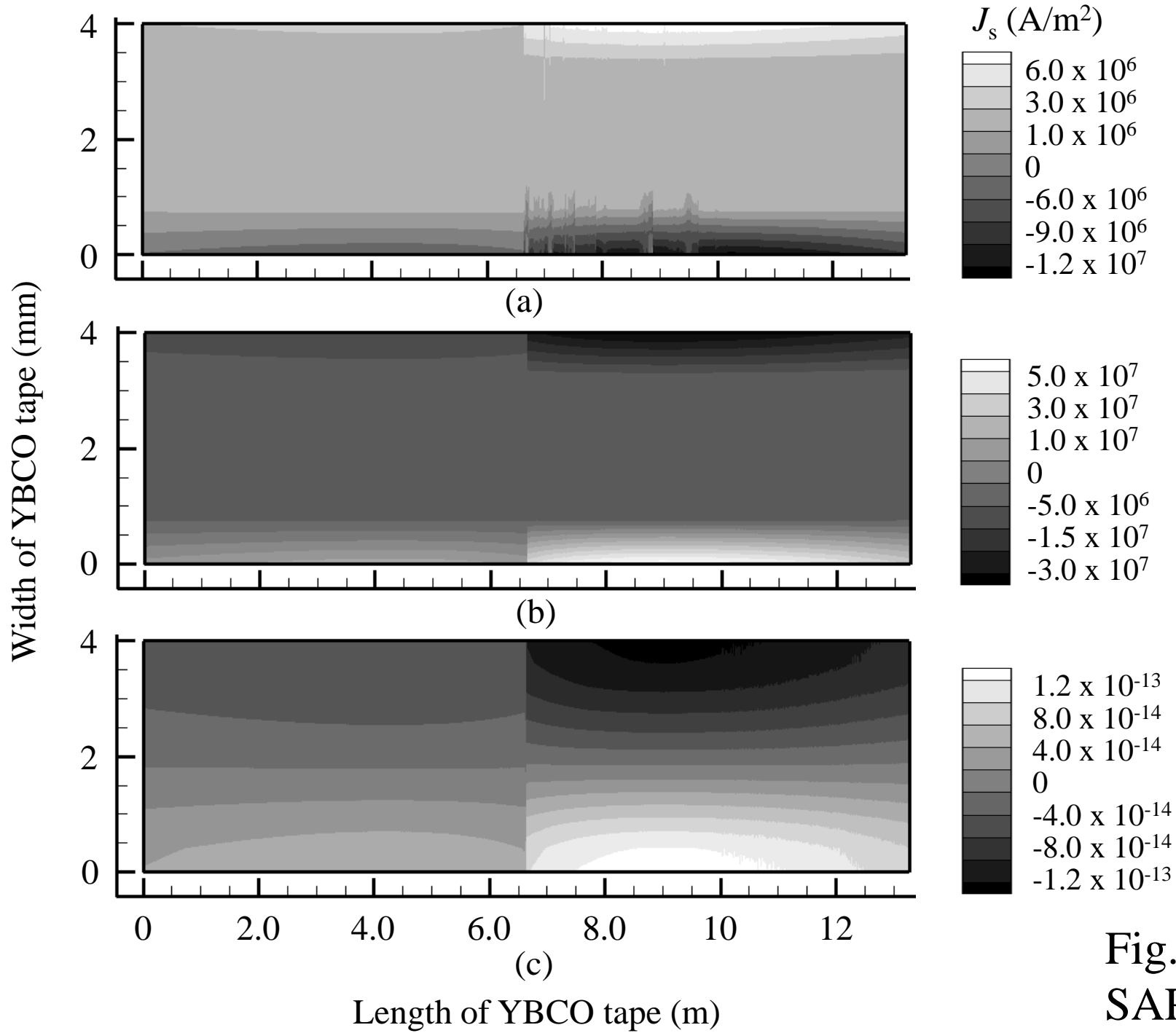


Fig. 9
SAP-51

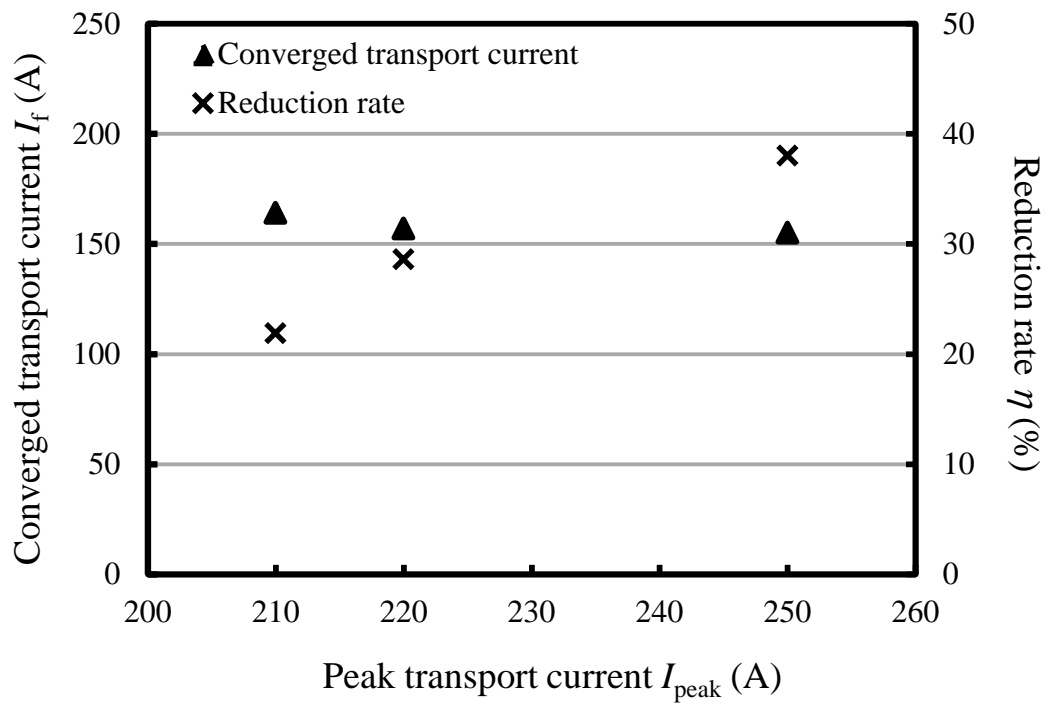


Fig. 10
SAP-51

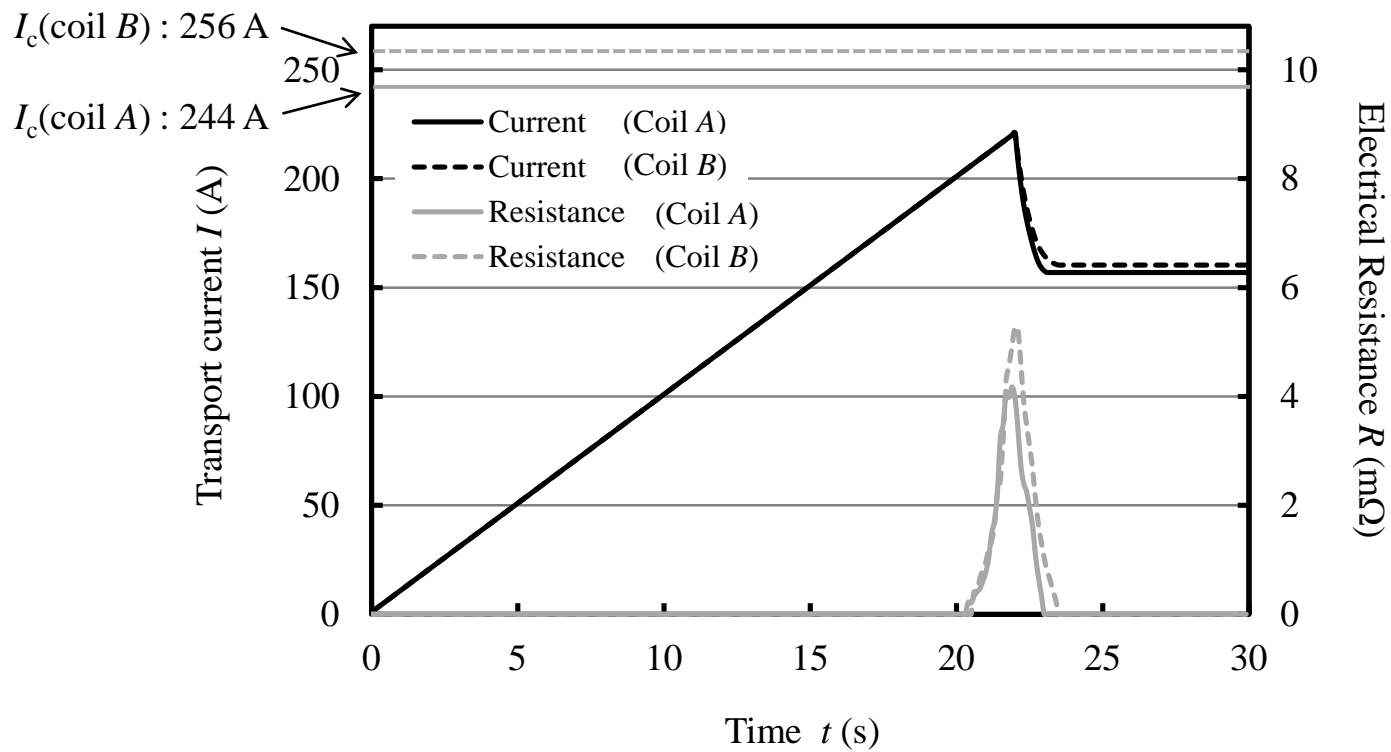


Fig. 11
SAP-51

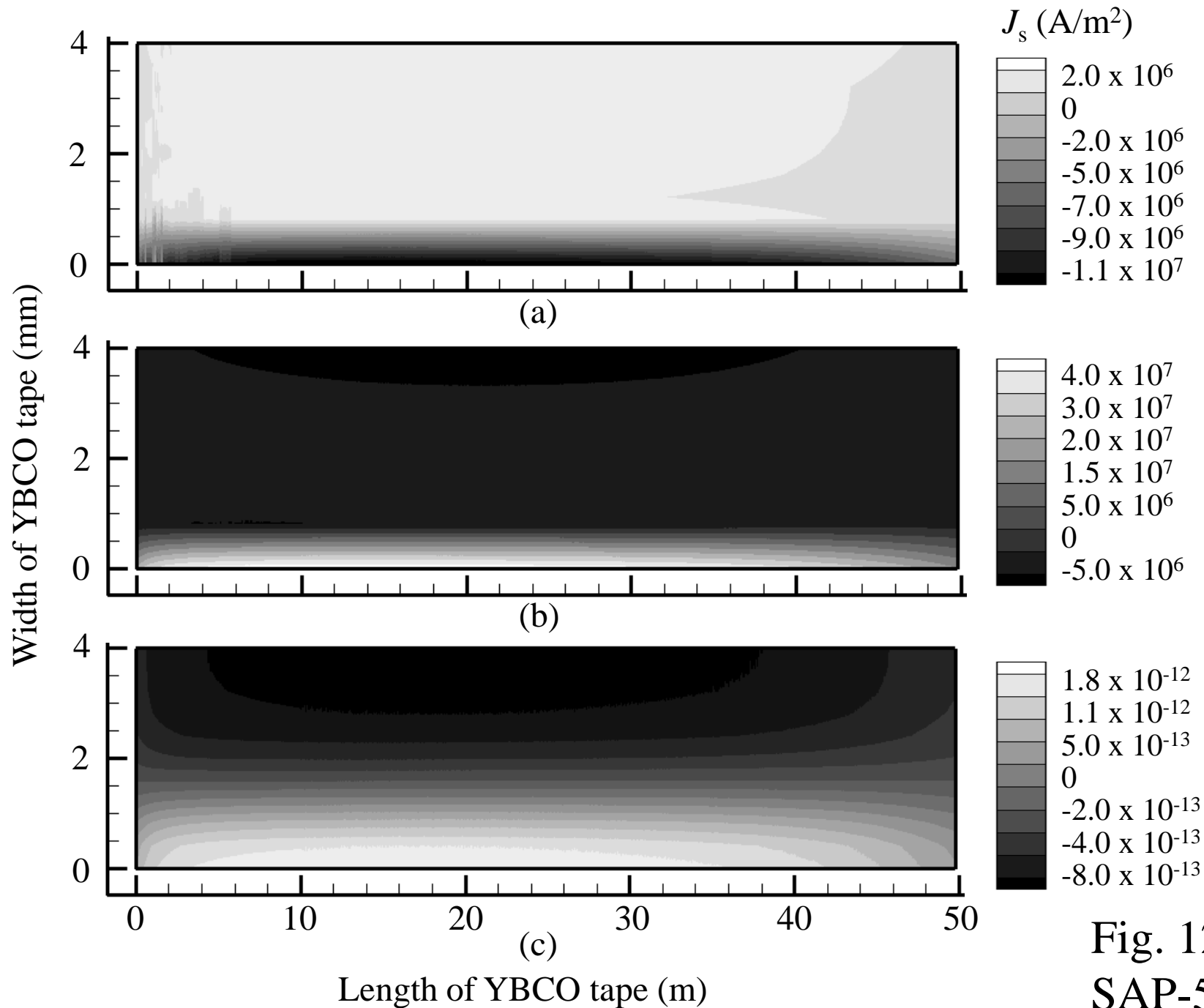


Fig. 12
SAP-51